Hindawi Publishing Corporation
Journal of Applied Mathematics
Volume 2014, Article ID 934250, 11 pages
http://dx.doi.org/10.1155/2014/934250

Research Article

Mathematical Model of Movement of the Observation and Tracking Head of an Unmanned Aerial Vehicle Performing Ground Target Search and Tracking

Izabela Krzysztofik and Zbigniew Koruba

Department of Applied Computer Science and Armament Engineering, Faculty of Mechatronics and Machine Design, Kielce University of Technology, 7 Tysiąclecia PP Street, 25-314 Kielce, Poland

Correspondence should be addressed to Izabela Krzysztofik; pssik@tu.kielce.pl

Received 24 April 2014; Revised 31 July 2014; Accepted 2 August 2014; Published 8 September 2014

Academic Editor: Zheping Yan

The paper presents the kinematics of mutual movement of an unmanned aerial vehicle (UAV) and a ground target. The controlled observation and tracking head (OTH) is a device responsible for observing the ground, searching for a ground target, and tracking it. The preprogrammed movement of the UAV on the circle with the simultaneous movement of the head axis on Archimedes' spiral during searching for a ground target, both fixed (bunkers, rocket missiles launching positions, etc.) and movable (tanks, infantry fighting vehicles, etc.), is considered. Dynamics of OTH during the performance of the above mentioned activities is examined. Some research results are presented in a graphical form.

1. Introduction

Due to the advantages of unmanned aerial vehicles (UAV) in relation to manned aircrafts, the multitask UAVs have become the basic equipment of a modern army [1]. They can carry out various tasks, such as aerial and radiolocation reconnaissance, observation of the battlefield, radioelectronic fight, adjustment of the artillery fire, target identification, laser indication of the target, assessment of the effects of striking other types of weapons, and imitation of air targets. UAVs can also have a wide civilian application, for example, observation and control of pipelines, electric tractions and road traffic. Because of that, more than 250 UAV models are developed and manufactured all over the world [2]. Many scientific institutions are engaged in developing and identifying models of dynamics and flight control of UAVs. For instance, papers [3, 4] present the comprehensive research on modelling the dynamics of flight of K100 UAV and Thunder Tiger Raptor 50 V2 Helicopter, respectively. Mathematical models of UAV with 6 degrees of freedom (6-DoF) introduced on the basis of the Newton's rules of dynamics were presented, whereas [5] presents the methodology of modelling the dynamics of UAV flight with the use of neural networks. Paper [6] presents the mathematical model and the experimental research on SUAVI. That vehicle can take off and land vertically. The model was carried out with the use of the Newton-Euler formalism. Moreover, the controllers for controlling the height and stabilizing the vehicle's location have been developed. Paper [7] describes the problem of flight dynamics of the UAV formation with the use of models with 3 and 6 degrees of freedom.

An operation of UAV during the completion of a task is a complex process requiring comprehensive technical means and systems. The control system of UAV is one of the most important systems. Its task is to measure, evaluate, and control flight parameters, as well as properly control the flight and observation systems. Thanks to the use of complex microprocessor systems, the comprehensive automation of the mentioned processes is possible. Formerly, during the completion of a mission it was necessary to maintain bilateral

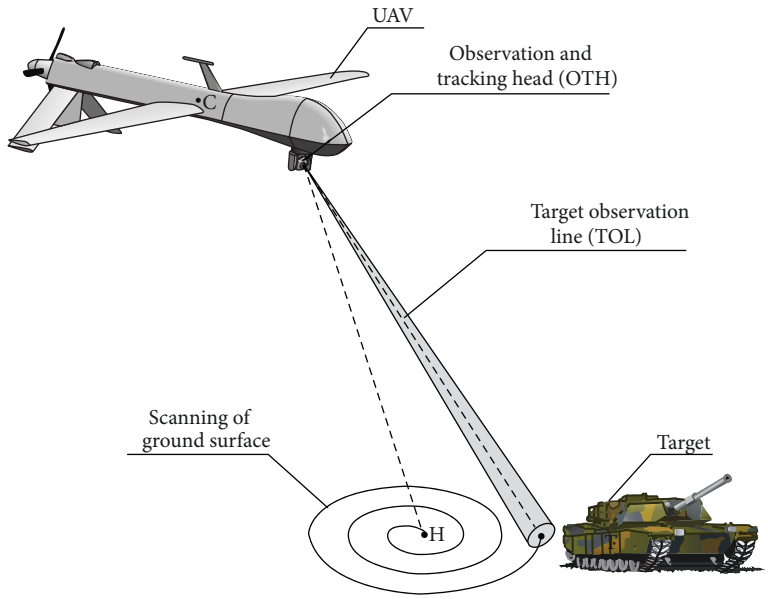

Figure 1: General view of the process of scanning the ground surface from UAV deck.

communications with the ground control point. In modern UAVs, autonomy plays an important role during detecting and tracking a ground target.

Paper [8] presents the model of the UAV autopilot and its sensors in the Matlab-Simulink environment for simulation research. Papers [9–11] pertain to planning and optimizing the trajectory of movement of the vehicle. The aspects of designing PID controllers for the systems of UAV flight control have been discussed in papers [12, 13].

From the quoted review of the literature it appears that the research mainly concentrates on UAV dynamics and control, without the consideration of the model of movement of the observation and tracking head (OTH) which is one of the most significant elements of the unmanned aerial vehicle. OTH is used for automatic searching for and tracking of targets intended for destruction [14]. This paper presents the mathematical model of kinematics of the movement of UAV, the ground target, and the dynamics of the controlled head located on the UAV deck. It needs to be emphasized that the problem of modelling, examining the dynamics, and control of such heads in the conditions of interferences from its base (deck of the manoeuvring UAV) is still topical. The paper examines this type of OTH with the built-in television and thermographic cameras and the laser illuminator.

2. Model of Movement Kinematics of UAV, OTH and Ground Target

General view of the process of searching for a target on the surface of the ground by OTH from UAV deck is shown in Figure 1, whereas the operation algorithm of OTH during scanning the ground surface and tracking a target detected on it is shown in Figure 2.

During the search for a ground target from UAV deck, the axis of OTH should perform the desired movements and circle strictly defined lines on the ground with the use of its extension. The optical system of OTH, having a certain viewing angle, may in this way encounter a light or infrared signal emitted by the moving object. Therefore, one should choose the kinematic parameters of mutual movement of UAV deck and OTH in such a way that the likelihood of detecting a target was the highest [15]. After locating a target, OTH goes to the tracking mode; that is, from that moment its axis has a specific location in space being pointed at the target.

Figure 3 shows the kinematics of mutual movement of the head axis and UAV during searching for a target on the ground surface. Individual coordinate systems have the following meaning:

$Ox_g y_g z_g$—Earth-fixed reference system,

$Cx_a y_a z_a$—coordinate system connected with target observation line (TOL),

$Cx_c y_c z_c$—movable coordinate system connected with UAV velocity vector.

The velocity of changing vector $\vec{R}$ in time, during searching for and tracking a target, is as follows:

$$\frac{d\vec{R}}{dt} = \Pi\left(t_o, t_d\right) \cdot \left(\vec{V}_c - \vec{V}_h\right) + \left[\Pi\left(t_d, t_t\right) + \Pi\left(t_t, t_e\right)\right] \cdot \left(\vec{V}_c - \vec{V}_t\right), \quad (1)$$

where $\vec{R}$ is vector of the mutual distance of points C and H (during scanning the space) or points C and T (during

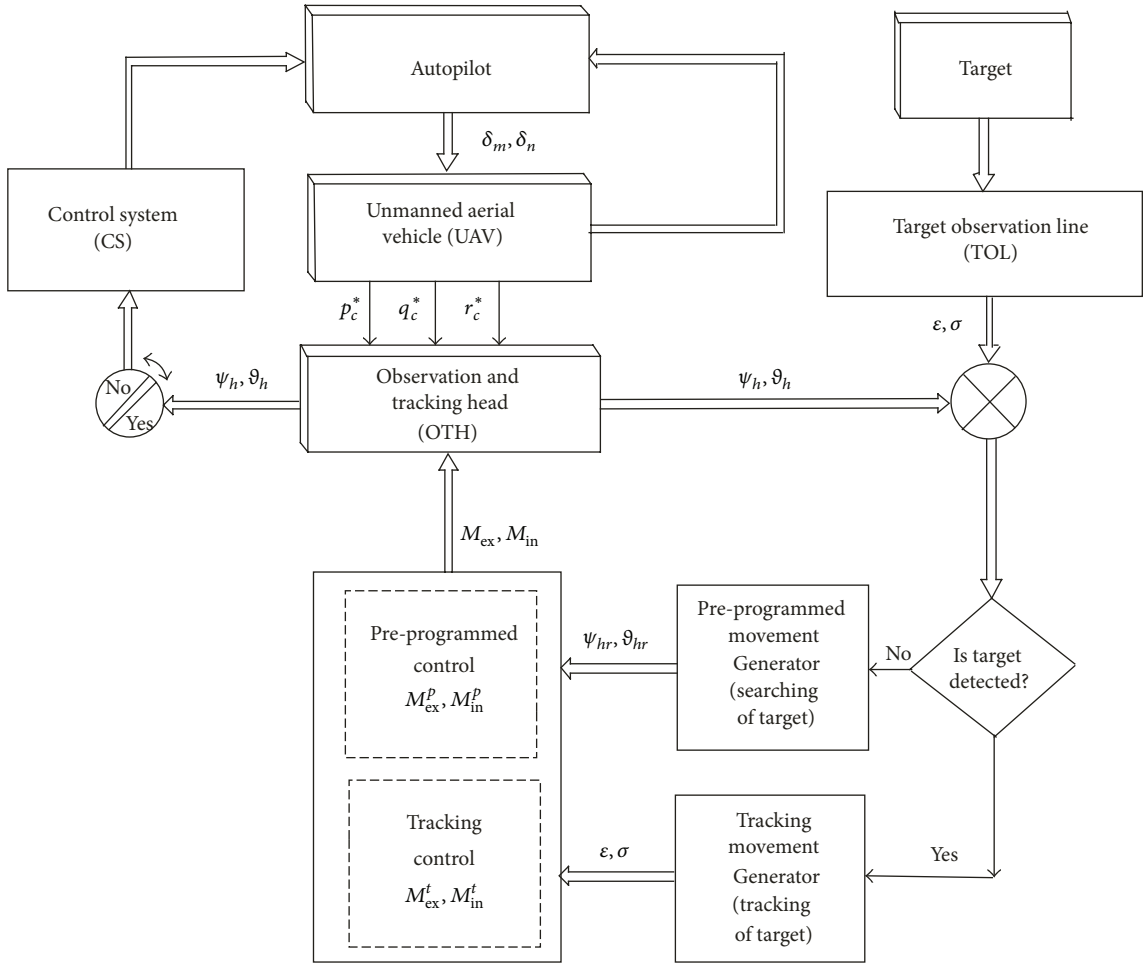

Figure 2: Diagram of operation of OTH mounted on UAV deck.

tracking); $\vec{V}_c, \vec{V}_h, \vec{V}_t$ are vectors of the velocity of movement of the centre of mass of UAV, of points H and T, respectively; $\Pi(t_o, t_d), \Pi(t_d, t_t), \Pi(t_t, t_e)$ are functions of rectangular impulse; t_o is the moment the scanning the ground is started; t_d is the moment a target is detected; t_t is the moment the tracking the target is started; t_e is the moment the scanning process and tracking the target is finished.

We project the left side of (1) on the axes of the coordinate system $Cx_a y_a z_a$ (Figure 3) connected with vector $\vec{R}$. In the result we get

$$\frac{d\vec{R}}{dt} = \frac{dR}{dt}\vec{i}_a + \begin{vmatrix} \vec{i}_a & \vec{j}_a & \vec{k}_a \\ \omega_{Rxa} & \omega_{Rya} & \omega_{Rza} \\ R & 0 & 0 \end{vmatrix} = \vec{i}_a \frac{dR}{dt} + \vec{j}_a R \frac{d\sigma}{dt} \cos\varepsilon - \vec{k}_a R \frac{d\varepsilon}{dt}, \tag{2}$$

where $\omega_{Rxa}, \omega_{Rya}, \omega_{Rza}$ are components of angular velocity of TOL and σ, ε are angles of deflection and inclination of vector $\vec{R}$.

Next, we project the right side of (1) (i.e., velocities $\vec{V}_c, \vec{V}_h$ and $\vec{V}_t$) on the axes of the system $Cx_a y_a z_a$ and get

$$\begin{aligned} \frac{dR}{dt} &= \Pi(t_o, t_d) \cdot (V_{cxa} - V_{hxa}) \\ &\quad + [\Pi(t_d, t_t) + \Pi(t_t, t_e)] \cdot (V_{cxa} - V_{txa}), \\ R\frac{d\sigma}{dt}\cos\varepsilon &= \Pi(t_o, t_d) \cdot (V_{cya} - V_{hya}) \\ &\quad + [\Pi(t_d, t_t) + \Pi(t_t, t_e)] \cdot (V_{cya} - V_{tya}), \\ R\frac{d\varepsilon}{dt} &= \Pi(t_o, t_d) \cdot (V_{cza} - V_{hza}) \\ &\quad + [\Pi(t_d, t_t) + \Pi(t_t, t_e)] \cdot (V_{cza} - V_{tza}). \end{aligned} \tag{3}$$

Individual components of velocity vectors $\vec{V}_c, \vec{V}_h$ and $\vec{V}_t$ in the system $Cx_a y_a z_a$ are as follows:

$$V_{cxa} = V_c [\cos\varepsilon \cos\gamma_c \cos(\sigma - \chi_c) + \sin\varepsilon \sin\gamma_c], \tag{4a}$$

$$V_{cya} = -V_c \cos\gamma_c \sin(\sigma - \chi_c), \tag{4b}$$

$$V_{cza} = V_c [\sin\varepsilon \cos\gamma_c \cos(\sigma - \chi_c) - \cos\varepsilon \sin\gamma_c], \tag{4c}$$

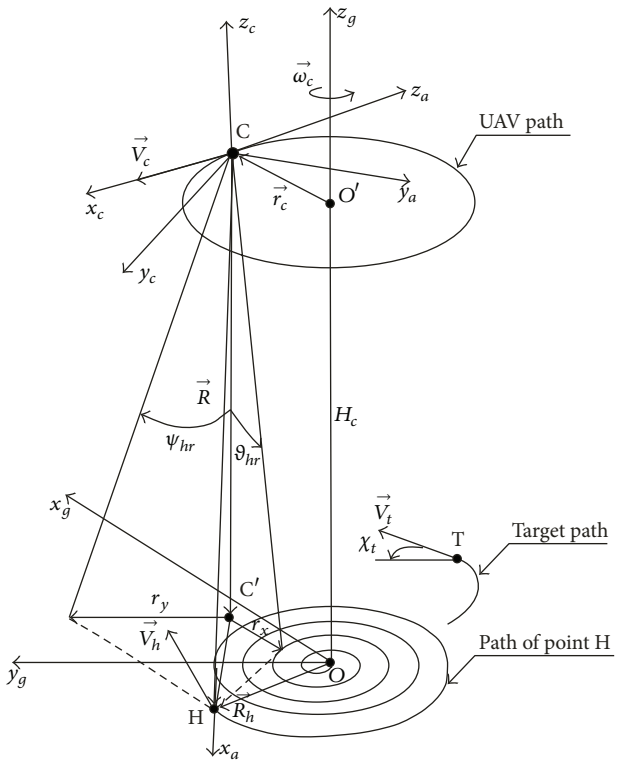

Figure 3: Kinematics of mutual movement of the head axis and UAV during scanning the ground surface.

$$V_{hxa} = V_h \left[\cos\varepsilon \cos\gamma_h \cos(\sigma - \chi_h) + \sin\varepsilon \sin\gamma_h\right], \quad (5a)$$

$$V_{hya} = -V_h \cos\gamma_h \sin(\sigma - \chi_h), \quad (5b)$$

$$V_{hza} = V_h \left[\sin\varepsilon \cos\gamma_h \cos(\sigma - \chi_h) - \cos\varepsilon \sin\gamma_h\right], \quad (5c)$$

$$V_{txa} = V_t \left[\cos\varepsilon \cos\gamma_t \cos(\sigma - \chi_t) + \sin\varepsilon \sin\gamma_t\right], \quad (6a)$$

$$V_{tya} = -V_t \cos\gamma_t \sin(\sigma - \chi_t), \quad (6b)$$

$$V_{tza} = V_t \left[\sin\varepsilon \cos\gamma_t \cos(\sigma - \chi_t) - \cos\varepsilon \sin\gamma_t\right], \quad (6c)$$

where χ_c, γ_c are UAV flight angles, χ_h, γ_h are angles of deflection and inclination of velocity vector of point H, and χ_t, γ_t are angles of deflection and inclination of velocity vector of point T.

For the simplification of reasoning, we assume that the movement of UAV, during searching and tracking, is done on a horizontal plane at a set altitude H_c, whereas the target and point H move in the ground plane. Then, we can assume that

$$\gamma_c = 0, \qquad \gamma_t = 0, \qquad \gamma_h = 0. \quad (7)$$

We mark that

$$r = R\cos\varepsilon \quad (8)$$

The derivative of that expression in relation to time is as follows:

$$\frac{dr}{dt} = \frac{dR}{dt}\cos\varepsilon - R\frac{d\varepsilon}{dt}\sin\varepsilon. \quad (9)$$

Let us substitute (4a)–(6c) into (3). Next, taking into account (7)–(9), (3) will have the following form:

$$\begin{aligned}\frac{dr}{dt} &= \Pi(t_o, t_d)\left[V_c \cos(\sigma - \chi_c^s) - V_h \cos(\sigma - \chi_h)\right] \\ &+ \Pi(t_d, t_t)\left[V_c \cos(\sigma - \chi_c^d) - V_t \cos(\sigma - \chi_t)\right] \\ &+ \Pi(t_t, t_e)\left[V_c \cos(\sigma - \chi_c^t) - V_t \cos(\sigma - \chi_t)\right],\end{aligned} \quad (10)$$

$$\begin{aligned}\frac{d\sigma}{dt} &= \Pi(t_o, t_d)\frac{V_c \sin(\sigma - \chi_c^s) - V_h \sin(\sigma - \chi_h)}{r} \\ &+ \Pi(t_d, t_t)\cdot\frac{V_c \sin(\sigma - \chi_c^d) - V_t \sin(\sigma - \chi_t)}{r} \\ &+ \Pi(t_t, t_e)\frac{V_c \sin(\sigma - \chi_c^t) - V_t \sin(\sigma - \chi_t)}{r},\end{aligned} \quad (11)$$

where r is mutual distance of points C and H (during scanning) or C and T (during tracking); χ_c^s is angle of deflection of UAV velocity vector during scanning the ground by the head; χ_c^d is angle of deflection of UAV velocity vector during the passage from preprogrammed flight to tracking flight; and χ_c^t is angle of deflection of UAV velocity vector during the flight tracking the detected target.

We demand that, at the moment of detecting the target, UAV automatically is starting the passage to the flight tracking the detected target; that is, it is moving at a set constant distance from the target $r_{c0} = R_{c0}\cos\varepsilon = \text{const}$ (in a horizontal plane at a constant altitude H_c).

If the mutual distance r of points C and T is different from r_{c0} then the angle of deflection of UAV velocity vector $\chi_c = \chi_c^d$ changes in accordance with the relationship:

$$\frac{d\chi_c^d}{dt} = a_c \cdot \operatorname{sign}(r_{c0} - r)\frac{d\sigma}{dt}, \quad (12)$$

where a_c is the set constant of proportional navigation.

After the fulfillment of the condition $r = r_{c0}$ the programme of angle change χ_c^t can be determined from (10):

$$\chi_c^t = \sigma - \arccos\left[\frac{V_t}{V_c}\cos(\sigma - \chi_t)\right]. \quad (13)$$

The path of UAV flight during scanning and tracking is as follows :

$$\frac{dr_c}{dt} = \Pi(t_o, t_d) V_c \cos(\theta_c - \chi_c^s) + \Pi(t_d, t_t) V_c \cos(\theta_c - \chi_c^d) + \Pi(t_t, t_e) V_c \cos(\theta_c - \chi_c^t), \tag{14a}$$

$$\frac{d\theta_c}{dt} = \Pi(t_o, t_d) \frac{V_c}{r_c} \sin(\theta_c - \chi_c^s) + \Pi(t_d, t_t) \frac{V_c}{r_c} \sin(\theta_c - \chi_c^d) + \Pi(t_t, t_e) \frac{V_c}{r_c} \sin(\theta_c - \chi_c^t), \tag{14b}$$

$$\begin{aligned} r_{cx} &= r_c \cos\theta_c, \\ r_{cy} &= r_c \sin\theta_c, \end{aligned} \tag{15}$$

where r_c is vector of location of UAV mass centre (point C) and θ_c is angle of deflection of vector r_c.

Path of movement of point H is as follows:

$$\frac{dR_h}{dt} = \Pi(t_o, t_d) V_h \cos(\theta_h - \chi_h), \tag{16a}$$

$$\frac{d\theta_h}{dt} = \Pi(t_o, t_d) V_h \sin(\theta_h - \chi_h), \tag{16b}$$

$$\begin{aligned} R_{hx} &= R_h \cos\theta_h, \\ R_{hy} &= R_h \sin\theta_h, \end{aligned} \tag{17}$$

where R_h is vector of location of point H and θ_h is angle of deflection of vector R_h.

Path of movement of the target is as follows:

$$\frac{dR_t}{dt} = \Pi(t_d, t_e) V_t \cos(\theta_t - \chi_t), \tag{18a}$$

$$\frac{d\theta_t}{dt} = \Pi(t_d, t_e) V_t \sin(\theta_t - \chi_t), \tag{18b}$$

$$\begin{aligned} R_{tx} &= R_t \cos\theta_t, \\ R_{ty} &= R_t \sin\theta_t, \end{aligned} \tag{19}$$

where R_t is vector of location of point T and θ_t is angle of deflection of vector R_t.

Desired angles $\vartheta_{hr}, \psi_{hr}$ and angular velocities $\dot{\vartheta}_{hr}, \dot{\psi}_{hr}$ of deflection of OTH axis can be determined from the following relationships:

$$\begin{aligned} \vartheta_{hr} &= \operatorname{arc}tg\frac{r_x}{H_c}, \qquad \frac{d\vartheta_{hr}}{dt} = \frac{H_c(dr_x/dt)}{H_c^2 + (r_x)^2}, \\ \psi_{hr} &= \operatorname{arc}tg\frac{r_y}{H_c}, \qquad \frac{d\psi_{hr}}{dt} = \frac{H_c(dr_y/dt)}{H_c^2 + (r_y)^2}, \end{aligned} \tag{20}$$

where

$$\begin{aligned} r_x &= r\cos\sigma, \qquad r_y = r\sin\sigma; \\ \frac{dr_x}{dt} &= \frac{dr}{dt}\cos\sigma - r\frac{d\sigma}{dt}\sin\sigma; \\ \frac{dr_y}{dt} &= \frac{dr}{dt}\sin\sigma + r\frac{d\sigma}{dt}\cos\sigma. \end{aligned} \tag{21}$$

Values (20) are used for determining the preprogrammed controls influencing the head.

2.1. Scanning the Ground Surface during UAV Flight on a Circle. We assume that during scanning the set area of the ground, UAV flight is at a constant altitude H_c in a horizontal plane on the circle of the set radius r_c with constant velocity V_c (Figure 3).

Then the preprogrammed UAV flight can be determined from the following relationships:

$$V_c = \omega_c \cdot r_c, \qquad \chi_c = \omega_c t. \tag{22}$$

At the same time, we control the head axis in such a way that it drawn on the surface of the ground a curve in the shape of Archimedean spiral with angular velocity

$$\omega_h = \frac{2\pi V_h}{\rho_h}. \tag{23}$$

Velocity V_h is to be chosen in such a way that OTH mounted on UAV deck could in the set time t_s scan densely enough the set surface of the area in the shape of a circle of the radius R_s.

If the angle of vision of the head's optical system amounts to ϕ_h then lens coverage embraces the surface similar in shape to a circle of the radius:

$$\rho_h = \frac{1}{2} H_c \phi_h. \tag{24}$$

After detecting a target at the moment t_d, UAV passes into the tracking flight according to the relationship (12), while the target is lit with a laser beam for the period of time t_l. Hence, the total time of the process of detecting, tracking, and lighting the target amounts to $t_e = t_d + t_l$.

3. The Model of Dynamics of the Controlled Observation and Tracking Head

A spatial model of dynamics of the head presented in Figure 4 was adopted for the paper. OTH comprises two basic parts: external frame and internal frame with camera. Movement of the head is determined with the use of two angles: angle of head deflection ψ_h and angle of head inclination ϑ_h [16].

The following coordinate systems, shown in Figure 5, have been introduced:

$Cx_dy_dz_d$—the movable system connected with the UAV deck,

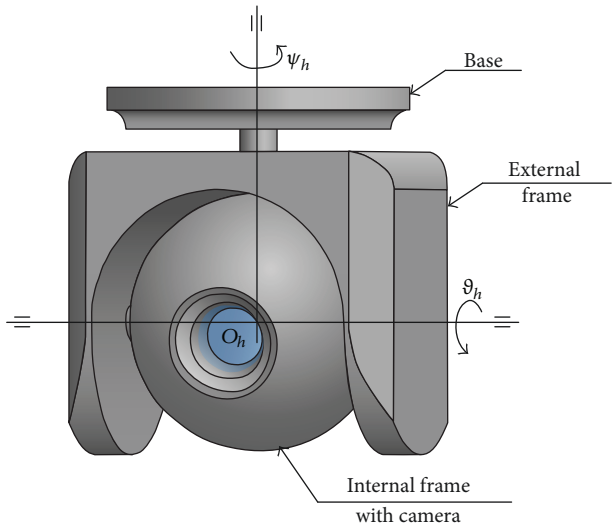

Figure 4: General view of the observation and tracking head.

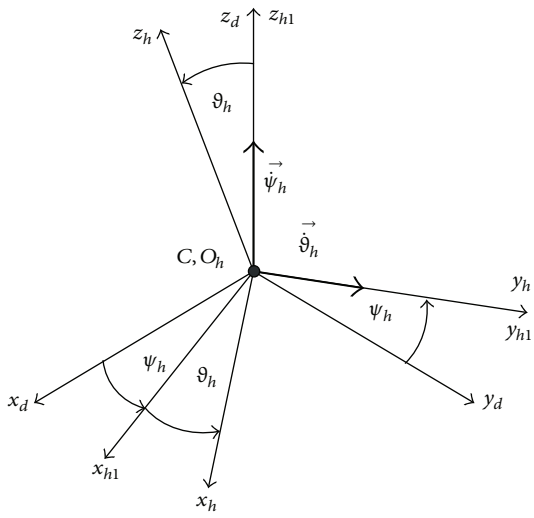

Figure 5: Transformations of the coordinate systems.

$O_h x_{h1} y_{h1} z_{h1}$—the movable system connected with the external frame of the head,

$O_h x_h y_h z_h$—the movable system connected with internal the frame of the head (including camera).

Components of angular velocity of the external frame of the head are

$$\omega_{x_{h1}} = p_c^* \cos\psi_h + q_c^* \sin\psi_h, \tag{25a}$$

$$\omega_{y_{h1}} = -p_c^* \sin\psi_h + q_c^* \cos\psi_h, \tag{25b}$$

$$\omega_{z_{h1}} = \dot{\psi}_h + r_c^*, \tag{25c}$$

where p_c^*, q_c^*, r_c^* are components of angular velocity of UAV.

Components of angular velocity of the internal frame of the head are

$$\omega_{x_h} = \omega_{x_{h1}} \cos\vartheta_h - \omega_{z_{h1}} \sin\vartheta_h, \tag{26a}$$

$$\omega_{y_h} = \omega_{y_{h1}} + \dot{\vartheta}_h, \tag{26b}$$

$$\omega_{z_h} = \omega_{x_{h1}} \sin\vartheta_h + \omega_{z_{h1}} \cos\vartheta_h. \tag{26c}$$

Components of linear velocity of displacement of mass centre of the external frame of the head are

$$V_{x_{h1}} = V_c \cos\psi_h, \tag{27a}$$

$$V_{y_{h1}} = -V_c \sin\psi_h, \tag{27b}$$

$$V_{z_{h1}} = 0. \tag{27c}$$

Components of linear velocity of displacement of mass centre of the internal frame of the head are

$$V_{x_h} = V_{x_{h1}} \cos\vartheta_h + l_h \omega_{y_{h1}} \sin\vartheta_h, \tag{28a}$$

$$V_{y_h} = V_{y_{h1}} + l_h \left(\omega_{z_{h1}} + \omega_{z_h}\right), \tag{28b}$$

$$V_{z_h} = V_{x_{h1}} \sin\vartheta_h - l_h \left(\omega_{y_{h1}} \cos\vartheta_h + \omega_{y_h}\right). \tag{28c}$$

Using the second order Lagrange equations, the following equations of the head movement have been derived:

$$\begin{aligned}
&J_{z_{h1}} \frac{d}{dt}\omega_{z_{h1}} - J_{x_h} \frac{d}{dt}\left(\omega_{x_h} \sin\vartheta_h\right) + J_{z_h} \frac{d}{dt}\left(\omega_{z_h} \cos\vartheta_h\right) \\
&\quad + m_{rw} l_h \frac{d}{dt}\left[V_{y_h}\left(1 + \cos\vartheta_h\right)\right] - \left(J_{x_{h1}} - J_{y_{h1}}\right)\omega_{x_{h1}}\omega_{y_{h1}} \\
&\quad - J_{x_h}\omega_{x_h}\omega_{y_{h1}} \cos\vartheta_h + J_{y_h}\omega_{y_h}\omega_{x_{h1}} - J_{z_h}\omega_{z_h}\omega_{y_{h1}} \sin\vartheta_h \\
&\quad + m_{\text{in}} l_h \left[V_{x_h}\omega_{x_{h1}} \sin\vartheta_h - V_{y_h}\omega_{y_{h1}} \sin\vartheta_h \right. \\
&\qquad \left. - V_{z_h}\omega_{x_{h1}}\left(1 + \cos\vartheta_h\right)\right] \\
&\quad + m_{\text{in}} l_h \left[V_{x_{h1}}\left(\omega_{z_{h1}} + \omega_{z_h}\right) + V_{y_{h1}}\omega_{y_h} \sin\vartheta_h\right] \\
&= M_{\text{ex}} + M_{\text{ex}}^g - M_{d\text{ex}}, \\
&J_{y_h} \frac{d}{dt}\omega_{y_h} - m_{\text{in}} l_h \frac{d}{dt} V_{z_h} + \left(J_{x_h} - J_{z_h}\right)\omega_{x_h}\omega_{z_h} \\
&\quad - m_{\text{in}} l_h \left[V_{y_h}\omega_{x_h} - V_{xh}\omega_{y_h}\right] = M_{\text{in}} + M_{\text{in}}^g - M_{d\text{in}},
\end{aligned} \tag{29}$$

where ψ_h, ϑ_h are angles of location of OTH axis in space; m_{in} is the mass of internal frame with camera; l_h is the distance of mass centre of internal frame (camera) from the centre of movement; $J_{x_{h1}}, J_{y_{h1}}, J_{z_{h1}}$ are moments of inertia of external frame; $J_{x_h}, J_{y_h}, J_{z_h}$ are moments of inertia of internal frame (with camera); $M_{\text{ex}}, M_{\text{in}}$ are moments of controlling forces influencing, respectively, external and internal frame; $M_{\text{ex}}^g, M_{\text{in}}^g$ are moments of the force of gravity influencing

respectively: external and internal frame; $M_{\text{ex}}^{g} = 0$; $M_{\text{in}}^{g} = m_{\text{in}} g l_h \cos \vartheta_h$; and $\vec{M}_{d\text{ex}}, \vec{M}_{d\text{in}}$ are moments of friction forces in the bearings of, respectively, external and internal frame.

We assume viscous friction:

$$M_{d\text{ex}} = \eta_{\text{ex}} \dot{\psi}_h; \qquad M_{d\text{in}} = \eta_{\text{in}} \dot{\vartheta}_h, \tag{30}$$

where η_{ex} is friction coefficient in suspension bearing of external frame and η_{in} is friction coefficient in suspension bearing of internal frame.

Control moments $M_{\text{ex}}, M_{\text{in}}$ of the head will be presented as follows [17–19]:

$$\begin{aligned} M_{\text{ex}} &= \Pi(t_o, t_d) \cdot M_{\text{ex}}^{p}(t) + \Pi(t_t, t_e) \cdot M_{\text{ex}}^{t}(t), \\ M_{\text{in}} &= \Pi(t_o, t_d) \cdot M_{\text{in}}^{p}(t) + \Pi(t_t, t_e) \cdot M_{\text{in}}^{t}(t), \end{aligned} \tag{31}$$

where $M_{\text{ex}}^{p}, M_{\text{in}}^{p}$ are preprogrammed control moments and $M_{\text{ex}}^{t}, M_{\text{in}}^{t}$ are tracking control moments.

Preprogrammed control moments $M_{\text{ex}}^{p}, M_{\text{in}}^{p}$, which set the head axis into the required motion, are determined from the following relationships:

$$\begin{aligned} M_{\text{ex}}^{p}(t) &= \Pi(t_o, t_d) \cdot \left[k_{\text{ex}}(\psi_h - \psi_{hr}) + h_{\text{ex}}(\dot{\psi}_h - \dot{\psi}_{hr})\right], \\ M_{\text{in}}^{p}(t) &= \Pi(t_o, t_d) \cdot \left[k_{\text{in}}(\vartheta_h - \vartheta_{hr}) + h_{\text{in}}(\dot{\vartheta}_h - \dot{\vartheta}_{hr})\right], \end{aligned} \tag{32}$$

where $k_{\text{ex}}, k_{\text{in}}$ are gain coefficients of the OTH control system and $h_{\text{ex}}, h_{\text{in}}$ are attenuation coefficients of the OTH control system.

Angles $\vartheta_{hr}, \psi_{hr}$ and their derivatives will be determined from the relationships (20).

At the moment when the target will appear in the head coverage, that is,

$$\left|\vec{R}_t - \vec{R}_h\right| \le \rho_h, \tag{33}$$

head control passes to the tracking mode.

Then, tracking control moments have the following form:

$$\begin{aligned} M_{\text{ex}}^{t}(t) &= \Pi(t_t, t_e) \cdot \left[k_{\text{ex}}(\psi_h - \sigma) + h_{\text{ex}}(\dot{\psi}_h - \dot{\sigma})\right], \\ M_{\text{in}}^{t}(t) &= \Pi(t_t, t_e) \cdot \left[k_{\text{in}}(\vartheta_h - \varepsilon) + h_{\text{in}}(\dot{\vartheta}_h - \dot{\varepsilon})\right]. \end{aligned} \tag{34}$$

Angles σ, ε will be determined from the relationships (3).

Coefficients $k_{\text{ex}}, k_{\text{in}}, h_{\text{ex}}, h_{\text{in}}$ are chosen in an optimum way due to the minimum deviation between the real and set path [15].

It should be emphasized that the mathematical model of movement of the controlled observation and tracking head described with (29) allows for conducting a number of simulation tests of searching for and tracking a ground target from the UAV deck. Thanks to that, one can know about the areas of stability and permissible controls with the influence of kinematic excitations from the UAV deck.

4. Results of Computer Simulations

The presented algorithms of control of the movement of OTH performing the search and tracking of a ground target from the UAV deck have been tested on the example of a hypothetical UAV system. The following parameters were adopted:

movement parameters of UAV

$$H_c = 1500\,\text{m}, \qquad r_c = 500\,\text{m}, \qquad V_c = 75\,\text{m/s}; \tag{35}$$

movement parameters of the head

$$\begin{aligned} t_s &= 10\,\text{s}, \qquad t_l = 20\,\text{s}, \\ R_s &= 500\,\text{m}, \qquad \phi_h = 1\ \text{deg}; \end{aligned} \tag{36}$$

movement parameters of the target

$$\begin{aligned} V_t &= 25\,\text{m/s}, \qquad \chi_t = \omega_t \cdot t, \\ \omega_t &= 0.025\,\text{rad/s}; \end{aligned} \tag{37}$$

mass parameters of the head

$$\begin{aligned} m_{\text{in}} &= 3.375\,\text{kg}, \qquad J_{x_{h1}} = 0.22\,\text{kgm}^2, \\ J_{y_{h1}} &= 0.114\,\text{kgm}^2, \qquad J_{z_{h1}} = 0.117\,\text{kgm}^2, \\ J_{x_h} &= 0.061\,\text{kgm}^2, \qquad J_{y_h} = 0.035\,\text{kgm}^2, \\ J_{z_h} &= 0.029\,\text{kgm}^2; \end{aligned} \tag{38}$$

the distance of mass centre of internal frame from the centre of movement

$$l_h = 0.002\,\text{m}; \tag{39}$$

friction coefficients in suspension bearings of the head

$$\eta_{\text{ex}} = \eta_{\text{in}} = 0.01\,\text{Nms/rad}. \tag{40}$$

Kinematic excitations of the base (UAV) were adopted in the following form:

$$\begin{aligned} p_c^* &= p_{c0}^* \sin(\nu \cdot t), \qquad q_c^* = q_{c0}^* \cos(\nu \cdot t), \\ r_c^* &= r_{c0}^* \sin(\nu \cdot t), \qquad p_{c0}^* = q_{c0}^* = r_{c0}^* = 0.5\,\text{rad/s}, \\ \nu &= 5\,\text{rad/s}. \end{aligned} \tag{41}$$

For nonoptimum control, regulator coefficients amounted to

$$\begin{aligned} k_{\text{ex}} &= -5.0, \qquad h_{\text{ex}} = -1.5, \\ k_{\text{in}} &= -5.0, \qquad h_{\text{in}} = -1.5. \end{aligned} \tag{42}$$

For optimum control, regulator coefficients amounted to

$$\begin{aligned} k_{\text{ex}} &= -20.0, \qquad h_{\text{ex}} = -5.0, \\ k_{\text{in}} &= -20.0, \qquad h_{\text{in}} = -5.0. \end{aligned} \tag{43}$$

Figure 6 presents the results of computer simulation of movement kinematics of UAV as well as the head axis during

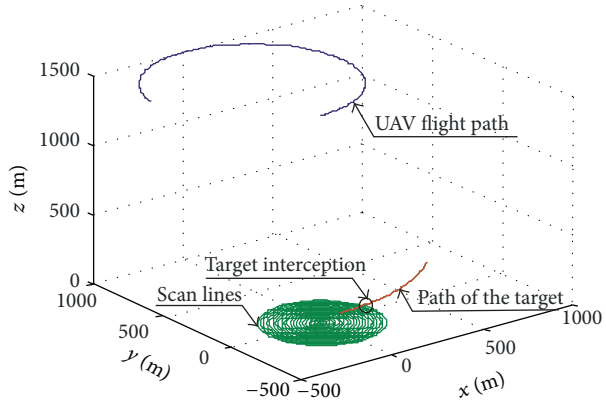

FIGURE 6: Path of movement of UAV, head axis, and the target during searching for and tracking the target.

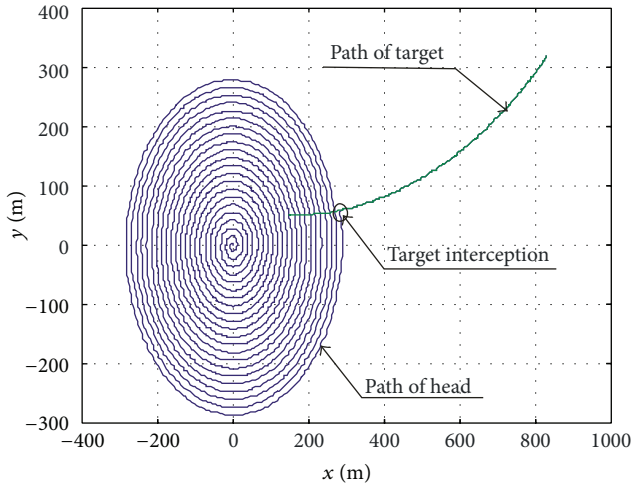

FIGURE 7: Path of movement of point H and the target on the surface of the ground.

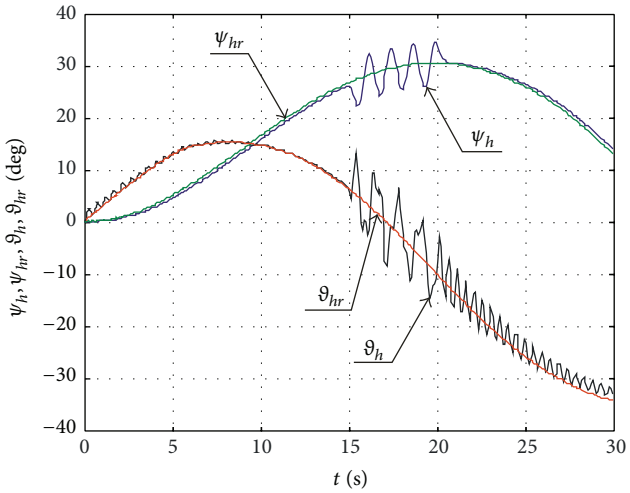

FIGURE 8: Time-dependent real ϑ_h, ψ_h and desired ϑ_{hr}, ψ_{hr} angles specifying the location of the head axis for nonoptimum controls with the influence of disturbances.

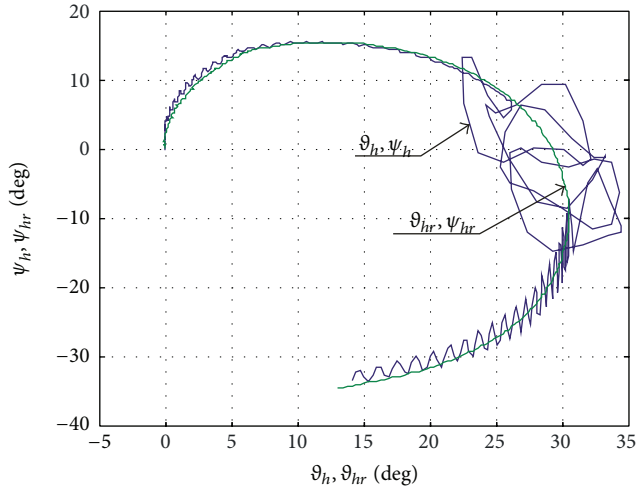

FIGURE 9: Real and desired trajectory of movement of the head axis for nonoptimum controls with the influence of disturbances.

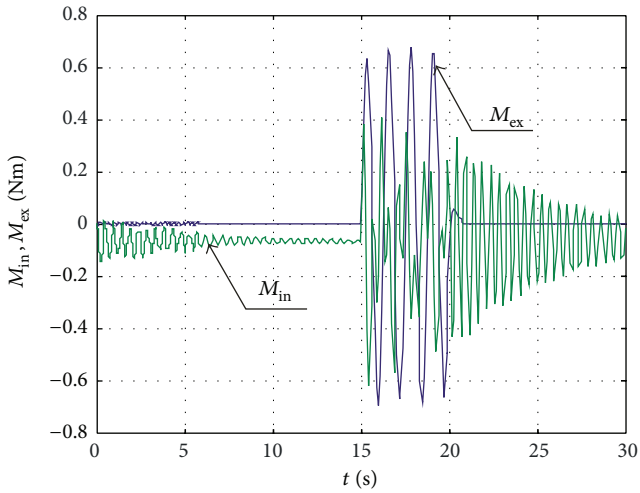

FIGURE 10: Time-dependent control moments M_{in} and M_{ex} for nonoptimum parameters of the regulator with the influence of disturbances.

searching the surface of the ground and tracking (laser lighting) a ground target.

Figure 7 presents the trajectory of movement of point H during scanning for and the movement of the target on the surface of the ground.

Figures 8–10 present the desired and the real angles of deflection and inclination of the head axis, as well as control moments for the case when the head is influenced by kinematic excitations from UAV deck and the parameters of the regulator are not optimum.

Figures 11, 12, and 13 present the desired and the real angles of deflection and inclination of the head axis, as well as control moments for the case when the head is not influenced by kinematic excitations from UAV deck and the parameters of the regulator are optimum.

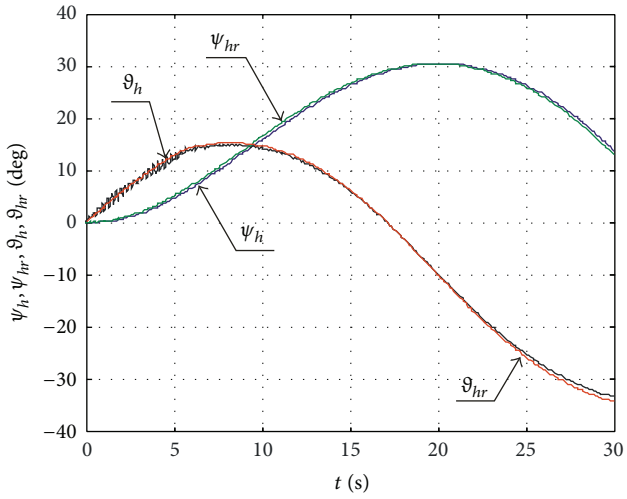

FIGURE 11: Time-dependent real ϑ_h, ψ_h and desired ϑ_{hr}, ψ_{hr} angles specifying the location of the head axis for optimum controls without the influence of disturbances.

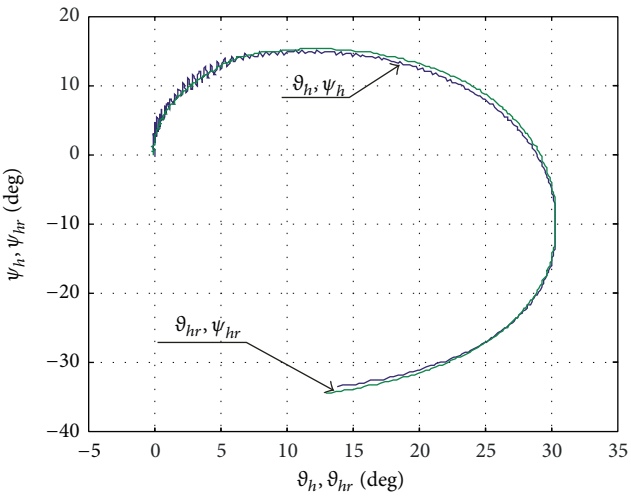

FIGURE 12: Real and desired trajectory of movement of the head axis for optimum controls without the influence of disturbances.

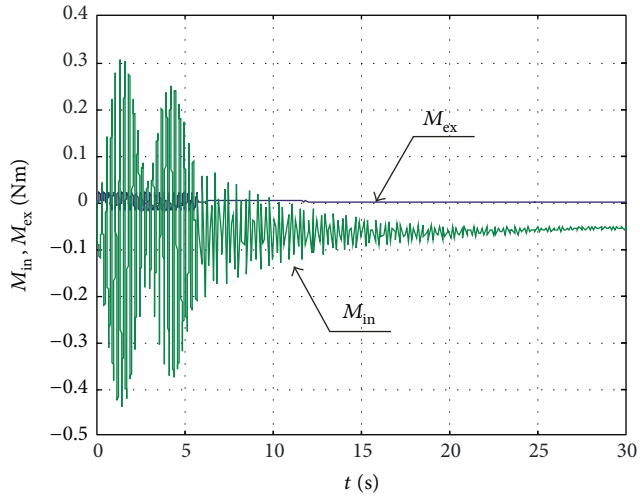

FIGURE 13: Time-dependent control moments M_{in} and M_{ex} for optimum parameters of the regulator without the influence of disturbances.

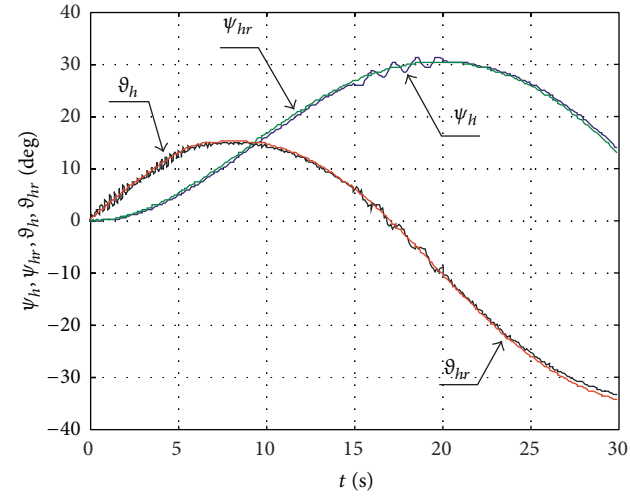

FIGURE 14: Time-dependent real ϑ_h, ψ_h and desired $\vartheta_{hr}, \psi_{hr}$ angles specifying the location of the head axis for optimum controls with the influence of disturbances.

Figures 14–16 present the desired and the real angles of deflection and inclination of the head axis, as well as control moments for the case when the head is influenced by kinematic excitations from UAV deck and the parameters of the regulator are optimum.

Kinematic excitations from UAV deck adversely affect the operation of the head. It can particularly be seen in Figures 11 and 14. In case of the nonoptimum choice of the parameters of the regulator, the deviations of the head axis from the set location are particularly visible (Figures 8 and 9). Smaller values of deviations can of course be achieved for optimum head controls (Figures 14 and 15). Control moments take small values.

From the presented theoretical analysis and the simulation research of the process of scanning by OTH from UAV deck of the surface of the ground and then tracking the detected ground target, it can be inferred that

(i) it is possible to search for a target on the area of any size, which is only limited to the durability and range of UAV flight;

(ii) scanning is sufficiently precise;

(iii) the programme of scanning the surface of the ground is simple;

(iv) there occur relatively small values of OTH axis angle deviations from the nominal position;

(v) full autonomy of UAV during the mission of searching and laser lighting of the detected ground target secures the point of control against detection and destruction by an enemy;

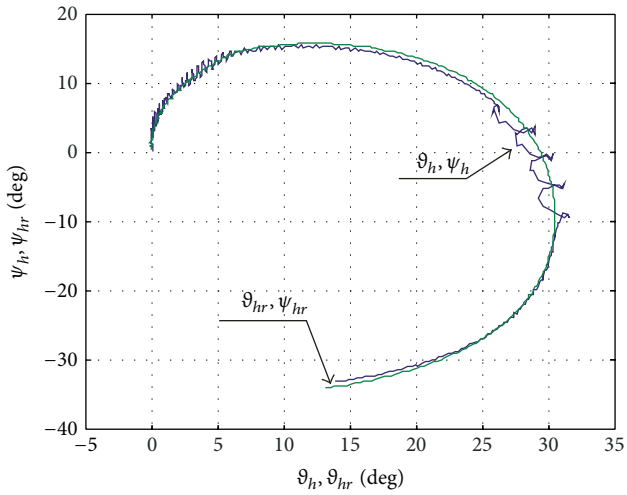

FIGURE 15: Real and desired trajectory of movement of the head axis for optimum controls with the influence of disturbances.

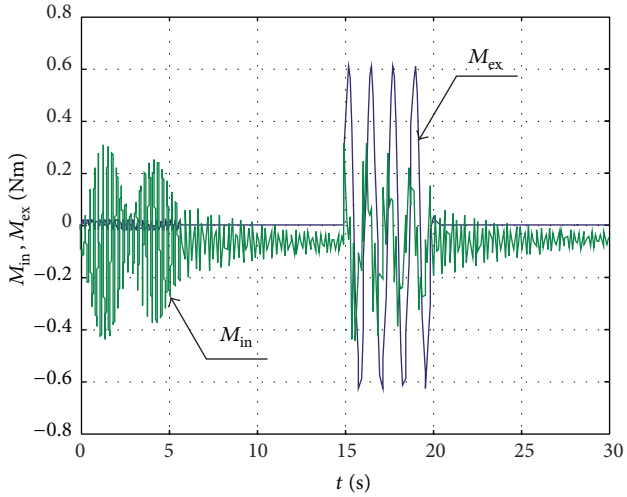

FIGURE 16: Time-dependent control moments M_{in} and M_{ex} for optimum parameters of the regulator without the influence of disturbances.

(vi) the interference of an operator in controlling UAV may only be limited to cases of the vehicle's total coming off from the set path or the loss of the target from OTH lens coverage (due to gusts of wind, explosions of missiles, etc.). Hence, the possibility of automatic sending of information about such occurrences to the control point and the possible taking of control over UAV flight by the operator should be introduced.

5. Conclusion

The considerations presented in this paper will allow us to conduct the research on the dynamics of OTH when manoeuvring UAV on which this device is mounted. It may enable the construction engineers to choose such parameters of OTH so that the transient processes occurring in the conditions of kinematic influence of UAV deck and at the moment of passing from scanning to tracking mode were minimized and disappeared in the shortest possible time.

Conflict of Interests

The authors declare that there is no conflict of interests regarding the publication of this paper.

Acknowledgment

The work reported herein was undertaken as part of a research project supported by the National Centre for Research and Development over the period 2011–2014.

References

[1] R. Austin, *Unmanned Aircraft Systems: UAVS Design, Development and Deployment*, John Wiley & Sons, Chichester, UK, 2010.

[2] F. Kamrani and R. Ayani, *UAV Path Planning in Search Operations, Aerial Vehicles*, InTech, 2009, edited by T. M. Lam.

[3] X. Q. Chen, Q. Ou, D. R. Wong et al., "Flight dynamics modelling and experimental validation for unmanned aerial vehicles," in *Mobile Robots-State of the Art in Land, Sea, Air, and Collaborative Missions*, X. Q. Chen, Ed., InTech, 2009.

[4] S. Bhandari, R. Colgren, P. Lederbogen, and S. Kowalchuk, "Six-DoF dynamic modeling and flight testing of a UAV helicopter," in *Proceedings of the AIAA Modeling and Simulation Technologies Conference*, pp. 992–1008, San Francisco, Calif, USA, August 2005.

[5] J. Manerowski and D. Rykaczewski, "Modelling of UAV flight dynamics using perceptron artificial neural networks," *Journal of Theoretical and Applied Mechanics*, vol. 43, no. 2, pp. 297–307, 2005.

[6] K. T. Öner, E. Çetinsoy, E. Sirimoğlu et al., "Mathematical modeling and vertical flight control of a tilt-wing UAV," *Turkish Journal of Electrical Engineering and Computer Sciences*, vol. 20, no. 1, pp. 149–157, 2012.

[7] T.-V. Chelaru, V. Pana, and A. Chelaru, "Flight dynamics for UAV formations," in *Proceedings of the 10th WSEAS International Conference on Automation & Information*, pp. 287–292, 2009.

[8] P. Kanovsky, L. Smrcek, and C. Goodchild, "Simulation of UAV Systems," *Acta Polytechnica*, vol. 45, no. 4, pp. 109–113, 2005.

[9] H. Ergezer and K. Leblebicioglu, "Planning unmanned aerial vehicles path for maximum information collection using evolutionary algorithms," in *Proceedings of the 18th IFAC World Congress*, pp. 5591–5596, Milano, Italy, 2011.

[10] C. Sabo and K. Cohen, "Fuzzy logic unmanned air vehicle motion planning," *Advances in Fuzzy Systems*, vol. 2012, Article ID 989051, 14 pages, 2012.

[11] H. Chen, K. Chang, and C. S. Agate, "Tracking with UAV using tangent-plus-lyapunov vector field guidance," in *Proceedings of the 12th International Conference on Information Fusion (FUSION '09)*, pp. 363–372, Seattle, Wash, USA, July 2009.

[12] K. Turkoglu, U. Ozdemir, M. Nikbay et al., "PID parameter optimization of an UAV longitudinal flight control system," *Proceedings of World Academy of Science: Engineering & Technology*, vol. 2, no. 9, pp. 24–29, 2008.

[13] B. Kada and Y. Ghazzawi, "Robust PID controller design for an UAV flight control system," in *Proceedings of the World Congress on Engineering and Computer Science (WCECS '11)*, vol. 2, San Francisco, Calif, USA, October 2011.

[14] I. Moir and A. Seabridge, *Military Avionics Systems*, John Wiley & Sons, Chichester, UK, 2007.

[15] J. Awrejcewicz and Z. Koruba, *Classical Mechanics: Applied Mechanics and Mechatronics*, vol. 30, Springer, New York, NY, USA, 2012.

[16] I. Krzysztofik, "The dynamics of the controlled observation and tracking head located on a moving vehicle," *Solid State Phenomena*, vol. 180, pp. 313–322, 2012.

[17] Z. Koruba, "Optimal control of the searching and tracking head (Sth) for self propelled anti aircraft vehicle," *Solid State Phenomena*, vol. 180, pp. 27–38, 2012.

[18] R. Langton, *Stability and Control of Aircraft Systems*, John Wiley & Sons, Chichester, UK, 2007.

[19] J. E. Takosoglu, P. A. Laski, and S. Blasiak, "A fuzzy logic controller for the positioning control of an electro-pneumatic servo-drive," *Proceedings of the Institution of Mechanical Engineers I: Journal of Systems and Control Engineering*, vol. 226, no. 10, pp. 1335–1343, 2012.